Favipiravir Tautomers: A Novel Investigation of Quantum Chemical, QTAIM, RDG - NCI, Bioactivity, and Molecular Docking Studies

Natte Kavitha*, Munagala Alivelu

Department of Chemistry, Pingle Govt. College for Women, Warangal, Telangana, India

*Correspondence email : kavithanatte2008@gmail.com

ABSTRACT

In this study, the quantum calculations of Favipiravir tautomers were evaluated using the B3LYP method with the 6-311++G (d,p) basis set. The DFT calculations have been carried out the atomic polarizability tensor charge (APT), Local descriptor function. The nature of the molecular interactions within the molecule through hydrogen bonding has been investigated using reduced density gradient (RDG), Non - covalent interactions (NCI), and Atoms in molecules (AIM). Potential energy surface (PES) scanning of the above compound has been examined. The additional studies like Bioactivity scores were discussed. Docking studies were analyzed to predict the binding energy.

Keywords : AIM, RDG - NCI, ADMET, QSAR, Docking.

I. INTRODUCTION

Since the late year of 2019, COVID-19 has been spread almost all around the world and made major damage to public health [1]. Every day, the number of infected people and the death rate grows tremendously. As a result, there is a pressing need to find an effective vaccination, a medication that can be used to address COVID-19. Finding a novel medication is a lengthy procedure. As a result, existing medicinal compounds and their analogs with promising drug-like properties would be the best remedy for the COVID-19 pandemic.

Heterocycles are widely investigated for possible medicinal applications [2-3]. The pyrazine moiety is a prime part of many clinically used drugs, including anticancer, diuretic [4], antidiabetic, antithrombotic, antidepressants, or anti-infective agents, and offers many possibilities in drug development [5]. Pyrazine-2-carboxamide may be used in the treatment of multi-drug resistant tuberculosis, a major growing problem among HIV-infected patients [6], and has multiple mechanisms of action and as a prodrug, it is metabolized via mycobacterial enzyme pyrazinamidase to form pyrazinoic acid [7]. Pyrazinoic acid accumulates intracellularly and lowers pH in a mycobacterial cell, which guides the inhibition of membrane transport and energy depletion [8]. Favipiravir is an antiviral medication with a pyrazine structure that was developed by the Fujifilm group in Japan and has an action against a wide range of RNA viruses [9]. It has been more over-examined for different types of influenza in the last years [10]. In abundant recent works, Favipiravir has

been designed for experimental treatments of COVID-19, in which it has been recommended as a helpful drug for the purpose [11].

Computer-aided drug design (CADD) has recently been utilized successfully in drug discovery. This method requires substantially less effort, time, and money when compared to traditional approaches. Quantum chemical computations have already been proved to be an excellent tool for evaluating molecule characteristics [12-13]. A systematic analysis has been done to investigate the structural properties of Favipiravir tautomers besides exploring their biological activity.

A more complete quantum chemistry research of the title molecule is required after reviewing prior investigations [14-16]. This research will look at two tautomeric structures 1 and 2 (Fig. 1) carried out using the DFT (B3LYP) method. Molecular properties such as APT charges, and Local reactivity descriptor properties have been calculated for both the tautomers. The Natural bond orbital study is used to estimate the stability of a molecule derived from hyper conjugative interaction and charged delocalization. AIM, NCI, and RDG here, this study aims to investigate hydrogen bond interaction within the molecule. Potential energy surface scan and local reactivity descriptor properties have been calculated for the Favipiravir. We created structural analogs of favipiravir (compounds 3 and 4) to target the virus in our work. The physicochemical properties of structural analogs of Favipiravir as a potential COVID-19 medicine were investigated using multiple computational methodologies (Bioactivity studies) in this work. Molecular docking studies are also explained to establish Favipiravir tautomer's biological activity.
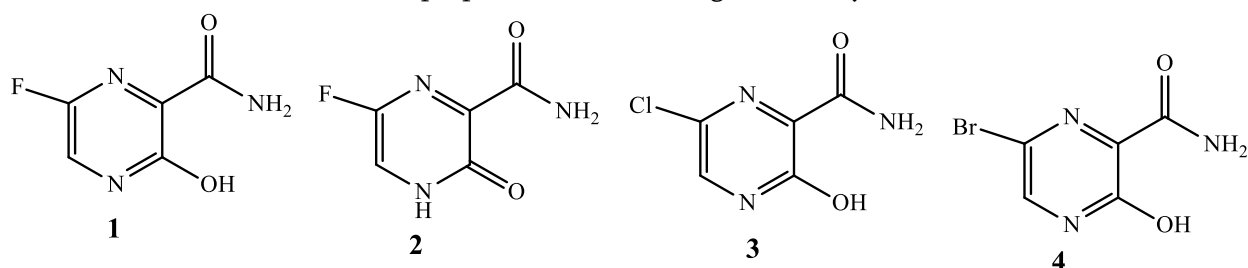

Fig.1. Structures of Favipiravir tautomer - I (1), tautomer - II (2), Cl - analog (3), and Br - analog (4).
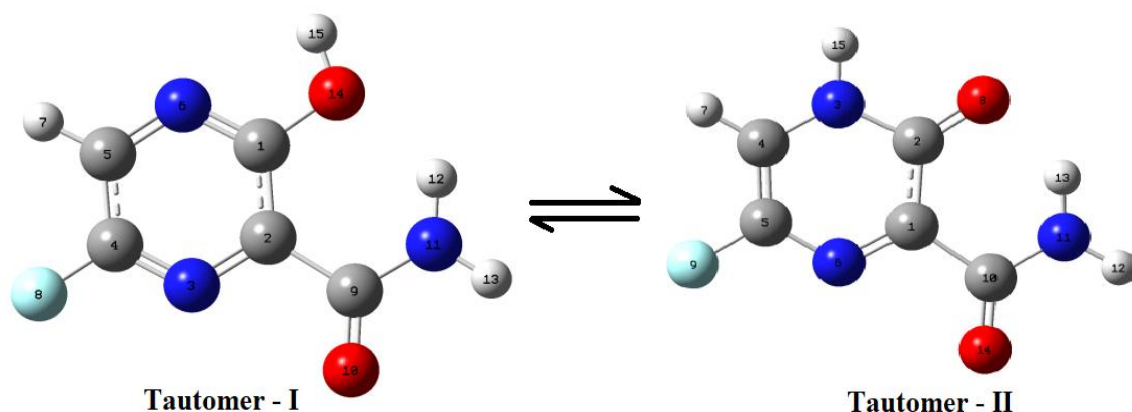

Fig. 2. Optimized geometric tautomeric structures with atom numbering of Favipiravir tautomer - I and tautomer - II.

II. THEORETICAL CALCULATIONS

Gaussian 09 software program package was used for theoretical calculation [17]. The quantum chemical calculations were accomplished by applying the density functional theory method with the three-parameter hybrid functional (B3) for the interchange part and the Lee-Yang-Par (LYP) correlation function with 6-311++G (d,p) basis set [18-19]. The optimized structural parameters were utilized in the calculations of DFT methods. Natural Bond Orbital (NBO) analysis [20] using B3LYP/6-311++G(d,p) level to understand hyper conjugative interactions and charge delocalization. Using the theory of Bader's quantum theory of atoms-in-molecules (QTAIM) framework [21], many topological parameters were deliberated by the means of the Multiwfn program [22]. The non-covalent interactions and strong repulsions in the molecule is resolved using reduced density gradient (RDG) analysis. Finally, the results were visualized using the VMD program [23-24]. Bioactivity scores were explored with molinspiration engine v2018.03 and the results proved them as safer drugs. Molecular docking studies were carried out using the Autodock 4.2.6 software package [25] and the docking results were visualized using Biovia discovery studiovisualizer 3.5 [26].

III. RESULTS AND DISCUSSION

3.1 Natural bond orbital (NBO) analysis

The NBO studies give information about the transfer of electrons from one place to another place i.e. donor NBO to acceptor NBO [27]. The strength of the acceptor interaction can be illumination from the interaction energy E(2). Using the equation [28-29] the E(2) can be determined. The stabilization energy E(2) associated with the i to j delocalization, for all donor NBO(i) and acceptor NBO(j), is calculated as

$$E(2) = \Delta E_{ij} = [q_i \, (F_{ij})^2]/ [\varepsilon_i - \varepsilon_j]$$

Where q_i is the ith donor orbital occupancy, ε_i, ε_j are diagonal elements (orbital energies) and F_{ij} is the off-diagonal element corresponding with NBO matrix. The huge E value indicates more intensive interaction between electron donors and electron acceptors, i.e., the increased donating propensity from electron donors to electron acceptors and significant the extent of conjugation of the entire system.

In the present study, the NBO analysis of Favipiravir tautomer molecules shows six types of transitions such as strong σ–σ*, n–σ*, n–π*, π–π*, σ–π*, π*–π* the hyper conjugative intramolecular interactions constructed by orbital interaction between bonding C–C, C–N, C–O, and C–F antibonding C–F, C–C, C–N, C–O and the bonding of lone pair atoms like N, O, F with C–N, C–O, C–F and N–H, antibonding orbitals C–C contact with antibonding orbitals of C–O which give an intra-molecular electron density delocalization and initiate the stability of a system.

All the interactions of the title compound tautomers were given in **Table 2.** From the table we obtained, the highest interaction from π*of C1☐C2 to π* C9☐O10 100.71 kcal/mol which donates the more stabilization in the tautomer - **I** molecule. The most important interactions from π C5☐N6 to π* C1☐C2 is 25.89 kcal/mol, π of C1☐C2 and N3☐C4 to anti-bonding of π* of N3☐C4 and C1☐C2 are 24.03 and 25.01 kcal /mol in this investigated molecule. The σ electron delocalization is considerable around C5-H7 bond and is diffuse to σ*antibonding of C1-N6 energy 4.62 kcal/mol. The electron delocalization energies are 3.95, 3.37 and 3.30 kcal/mol are due to the σ electron delocalization C2-N3, N11-H12, and C5-H7 that is diffuse to σ* anti-bonding of C4-F8, C9-O10 and N3-C4. Lone pair around LP (1) N11 is distributed to π* anti-bonding C9-O10 and LP(2) O10 distristributed to π* C9-N11 with stabilization energy 25.25 and 23.20 kcal/mol, whereas that around LP(3) F8 is distributed to π* antibonding N3-C 4 with stabilization energy 21.49 kcal/mol.

The tautomer - **II** shows the highest interactions from π*of C2-O9 to π* C1-N6 and π*C1-N6 to π* C10-O11 with stabilization energy 128.07 kcal/mol and 105.32 kcal/mol. The σ electron displacement is considerable around the C4-H7 bond and is diffuse to σ*antibonding of C5-N6 energy 5.24 kcal/mol. The electron delocalization energies are 4.25 and 3.67 kcal/mol are due to the σ electron delocalization C1-C10 and N3-C4, which is diffuse to σ* anti-bonding of

C5-N6 and C5-F8. Lone pair around LP(1) N12 is distributed to π* anti-bonding C10-O11 and LP(2) O9 distristributed to σ* anti-bonding C2-N3 with stabilization energy of about 25.70 and 25.54 kcal/mol, whereas that around LP(3) F8 is distributed to π* antibonding C4-C5 with stabilization energy 19.50 kcal/mol. As seen in the NBO analysis, the highest energy interactions were seen in tautomer - **II**.

Table 1. Second order perturbation theory analysis of Fock matrix in NBO basis for Favipiravir tautomer - **I** and tautomer - **II** at B3LYP/6–311++G (d, p) level of theory.

Donor (i)	Type	ED/e	Acceptor (j)	Type	Ed/e	E(2)[a]	E(i) -E(j)[b]	f(i,j)[c]
C1-C2	σ	1.98175	C1-C6	σ*	0.026	2.52	1.32	0.052
			C2-N3	σ*	0.01443	2.22	1.34	0.049
			C2-C9	σ*	0.0856	1.24	1.11	0.034
			C9-O10	σ*	0.01015	1.17	1.3	0.035
			014-H15	σ*	0.00841	1.06	1.16	0.031
C1-C2	π	1.55916	C1-C2	π *	0.36993	0.52	0.29	0.011
			N3-C4	π *	0.38581	24.03	0.28	0.074
			C5-N6	π	0.37261	21.93	0.28	0.071
			C9-O10	π *	0.23346	13.55	0.3	0.06
			O14-H15	π *	0.00841	0.51	0.7	0.019
C1-N6	σ	1.9864	C1-C2	σ*	0.04954	2.65	1.43	0.055
			C2-C9	σ*	0.0856	1.56	1.27	0.041
			C5-N6	σ*	0.01233	1.79	1.49	0.046
			C5-H7	σ*	0.02574	1.97	1.33	0.046
C1-O14	σ	1.99252	C2-N3	σ*	0.01443	1.64	1.45	0.44
			C5-N6	σ*	0.01233	2.24	1.45	0.051
C2-N3	σ	1.97657	C1-C2	σ*	0.04954	2.42	1.42	0.053
			C1-O14	σ*	0.05797	2.57	1.15	0.049
			C2-C9	σ*	0.0856	1.49	1.26	0.039
			N3-C4	σ*	0.02813	1.78	1.47	0.046
			C4-F8	σ*	0.06518	3.95	1.15	0.061
			C9-N11	σ*	0.06964	1.1	1.24	0.033
C2-C9	σ	1.97853	C1-C2	σ*	0.04954	0.98	1.17	0.03
			C1-N6	σ*	0.026	2.58	1.22	0.05
			C2-N3	σ*	0.01443	1.54	1.24	0.039
			N3-C4	σ*	0.02813	3.28	1.12	0.057

			N11-H13	σ*	0.00688	1.09	1.11	0.031
N3-C4	σ	1.9865	C2-N3	σ*	0.01443	1.85	1.48	0.047
			C2-C9	σ*	0.0856	3.21	1.26	0.058
			C4-H5	σ*	0.04798	2.11	1.4	0.049
			C5-H7	σ*	0.02574	0.96	1.32	0.032
N3-C4	π	1.0784	C1-C2	π *	0.03699	25.01	0.34	0.084
			C5-N6	π *	0.37261	17.05	0.33	0.068
C4-C5	σ	1.99014	N3-C4	σ*	0.02813	2.34	1.32	0.05
			C5-N6	σ*	0.01233	1.11	1.33	0.034
			C5-H7	σ*	0.02574	0.93	1.17	0.03
C4-F8	σ	1.99564	C2-N3	σ*	0.01443	1.62	1.6	0.035
			C5-N6	σ*	0.01233	0.97	1.6	0.035
C5-N6	σ	1.97887	C1-N6	σ*	0.026	2.08	1.47	0.049
			C1-014	σ*	0.05797	4.67	1.15	0.066
			C4-C5	σ*	0.04798	1.2	1.4	0.037
			C4-F8	σ*	0.06518	2.36	1.15	0.047
			C5-H7	σ*	0.02574	0.92	1.32	0.031
C5-N6	π	1.73936	C1-C2	π *	0.03699	25.89	0.34	0.086
			N3-C4	π *	0.38581	14.82	0.33	0.064
C5-H7	σ	1.98259	C1-N6	σ*	0.026	4.62	1.13	0.065
			N3-C4	σ*	0.02813	3.3	1.13	0.055
			C4-F8	σ*	0.06518	0.73	0.81	0.022
			C5-N6	σ*	0.01233	0.87	1.14	0.028
C9-O10	σ	1.99622	C1-C2	σ*	0.04954	0.68	1.51	0.029
C9-O10	π	1.97643	C1-C2	π *	0.36993	4.75	0.34	0.039
C9-N11	σ	1.99427	C2-N3	σ*	0.01443	1.38	1.32	0.038
N11-H12	σ	1.97955	C9-O10	σ*	0.0105	3.37	1.18	0.056
			C9-O10	π *	0.23346	1.33	0.64	0.028
			O14-H15	σ*	0.00841	0.51	1.04	0.021
N11 –H13	σ	1.98391	C2-C9	σ*	0.0856	3.18	0.99	0.051
			C9-O10	σ*	0.01015	0.54	1.17	0.022
			C9-O10	π *	0.02335	0.79	0.64	0.021
O14-H15	σ	1.98692	C1-C2	σ*	0.04954	2.43	1.28	0.05
			C1-C2	π *	0.03699	0.87	0.76	0.025
LP N3	σ	1.86967	C1-C2	σ*	0.04954	9.99	0.86	0.85
			C1-O14	σ*	0.05797	0.78	0.59	0.02
			C2-C9	σ*	0.0856	4.61	0.71	0.052
			C4-C5	σ*	0.04798	8.96	0.85	0.079
			C4-F8	σ*	0.06518	9.61	0.59	0.069

LPN6	σ	1.88545	C1-C2	σ*	0.04954	9.61	0.88	0.083
			C1-014	σ*	0.05797	8.53	0.61	0.065
			C4-C5	σ*	0.04798	8.95	0.86	0.08
			C4-F8	σ*	0.06518	0.78	0.61	0.02
			C5-H7	σ*	0.02574	4.89	0.78	0.056
LPF8	σ	1.99126	N3-C4	σ*	0.02813	0.66	1.63	0.029
LPF8	π	1.96588	N3-C4	σ*	0.02813	8.3	0.99	0.081
			C4-C5	σ*	0.04798	5.92	0.92	0.066
LPF8	3	1.91702	N3-C4	π*	0.38581	21.49	0.41	0.091
LPO10	1	1.9813	C2-C9	σ*	0.0856	1.67	1.05	0.038
			C9-N11	σ*	0.06964	1.27	1.02	0.033
LPO10	2	1.87318	C2-C9	σ*	0.0856	18.21	0.6	0.094
			C9-N11	σ*	0.06964	23.2	0.57	0.104
LPN11	1	1.81832	C9-O10	π*	0.02335	25.25	0.34	0.084
			N11-H12	σ*	0.0159	0.58	0.8	0.02
LPO14	1	1.97145	C1-N6	σ*	0.026	5.03	1.2	0.069
			N11-H12	σ*	0.0159	4.92	1.1	0.066
			N11-H13	σ*	0.00688	0.66	1.09	0.024
LPO14	2	1.90001	C1-C2	σ*	0.04954	1.15	0.88	0.29
			C1-C2	π*	0.03699	17.33	0.35	0.075
			C1-N6	σ*	0.026	0.63	0.93	0.027
C1-C2	π*	0.03699	C9-O10	π*	0.02335	100.71	0.02	0.04
Tautomer - II								
C1-C2	σ	1.98451	C1-N6	σ*	0.01551	2.80	1.34	0.055
			C1-C10	σ*	0.08789	0.73	1.12	0.026
			C2-O9	σ*	0.01388	1.56	1.28	0.040
			N3-H15	σ*	0.01338	0.87	1.16	0.028
			C10-O11	σ*	0.00945	1.05	1.30	0.033
C1-N6	σ	1.98316	C1-C2	σ*	0.05489	1.92	1.42	0.047
			C1-C10	σ*	0.08789	1.43	1.27	0.039
			C2-O9	σ*	0.01388	1.71	1.43	0.044
			C5-F8	σ*	0.03841	1.93	1.16	0.042
			C10-N12	σ*	0.06848	1.05	1.25	0.033
C1-N6	π	1.82211	C1- N6	π*	0.19409	1.17	0.34	0.018
			C2-O9	π*	0.30843	20.44	0.32	0.075
			C4-C5	π*	0.20853	11.11	0.34	0.055
			C10-O11	π*	0.23625	9.79	0.35	0.053
C1-C10	σ	1.97153	C1-C2	σ*	0.05489	1.26	1.16	0.034
			C1-N6	σ*	0.01551	1.99	1.23	0.044

			C2-N3	σ*	0.08612	3.75	0.95	0.054
			C5-N6	σ*	0.04394	4.25	0.98	0.058
			N12-H13	σ*	0.00845	1.07	1.12	0.031
C2-N3	σ	1.98488	C1-C10	σ*	0.08789	1.63	1.12	0.039
			C4-H7	σ*	0.01207	1.82	1.18	0.041
C2-O9	σ	1.99315	C1-C2	σ*	0.05489	1.52	1.53	0.044
			C1-N6	σ*	0.01551	1.86	1.60	0.049
			N3-C4	σ*	0.01637	0.80	1.32	0.029
C2-O9	π	1.96645	C1-N6	π*	0.19409	8.79	0.37	0.053
			C2-O9	π*	0.30843	0.58	0.35	0.014
			N12-H14	σ*	0.01535	0.68	0.85	0.022
N3-C4	σ	1.97888	C2-O9	σ*	0.01388	2.73	1.28	0.053
			C4-C5	σ*	0.02447	0.60	1.32	0.025
			C5-F8	σ*	0.03841	3.67	1.00	0.054
N3-H15	σ	1.96811	C1-C2	σ*	0.05489	2.27	1.17	0.046
			C2-O9	σ*	0.01388	0.51	1.18	0.022
			C2-O9	π*	0.30843	1.22	0.64	0.027
			C4-C5	σ*	0.02447	1.53	1.23	0.039
			C4-C5	π*	0.20853	1.01	0.66	0.024
C4-C5	σ	1.99106	C1-N6	σ*	0.01551	0.55	1.37	0.025
			N3-H15	σ*	0.01338	0.86	1.19	0.029
			C4-H7	σ*	0.01207	1.27	1.21	0.035
			C5-N6	σ*	0.04394	0.89	1.12	0.028
C4-C5	π	1.84162	C1-N6	π*	0.19409	11.26	0.32	0.054
			N3-H15	σ*	0.01338	0.99	0.72	0.025
C4-H7	σ	1.98022	C2-N3	σ*	0.08612	2.02	0.87	0.038
			C4-C5	σ*	0.02447	1.08	1.14	0.031
			C5-N6	σ*	0.04394	5.24	0.90	0.062
			C5-F8	σ*	0.03841	0.93	0.82	0.025
C5-N6	σ	1.98057	C1-C10	σ*	0.08789	4.08	1.11	0.061
			C4-C5	σ*	0.02447	1.11	1.32	0.034
			C4-H7	σ*	0.01207	1.87	1.16	0.042
			C1-N6	σ*	0.01551	0.68	1.60	0.029
			N3-C4	σ*	0.01637	1.68	1.33	0.042
C5-F8	σ	1.99540	C1-N6	σ*	0.01551	0.68	1.60	0.029
			N3-C4	σ*	0.01637	1.68	1.33	0.042
C10-O11	σ	1.99593	C1-C2	σ*	0.05489	0.78	1.50	0.031
			C1-N6	π*	0.19409	5.21	0.34	0.039
C10-N12	σ	1.99394	C1-N6	σ*	0.01551	1.44	1.31	0.039
N12-H13		1.98298	C1-C10	σ*	0.08789	3.29	0.98	0.052
			C10-O11	σ*	0.00945	0.51	1.17	0.022

			C10-O11	π *	0.23625	0.84	0.63	0.022
N12-H14	σ	1.97891	C10-O11	σ*	0.00945	3.38	1.17	0.056
			C10-O11	π *	0.23625	1.32	0.63	0.027
LP(1)N3		1.71245	C2-O9	π *	0.30843	23.26	0.36	0.083
			N3-H15	σ*	0.01338	1.37	0.79	0.032
			C4-C5	π *	0.20853	16.44	0.38	0.072
LP(1)N6		1.91339	C1-C2	σ*	0.05489	9.53	0.88	0.082
			C1-C10	σ*	0.08789	3.36	0.73	0.044
			C4-C5	σ*	0.02447	5.05	0.94	0.063
			C5-F8	σ*	0.03841	3.85	0.61	0.044
LP(1)F8		1.99004	C4-C5	σ*	0.02447	1.22	1.62	0.040
			C5-N6	σ*	0.04394	0.90	1.38	0.032
LP(2)F8		1.95655	N3-C4	σ*	0.01637	0.52	0.74	0.018
			C4-C5	σ*	0.02447	5.04	1.00	0.064
			C5-N6	σ*	0.04394	10.46	0.76	0.080
LP(3)F8		1.92739	C4-C5	π *	0.20853	19.50	0.42	0.084
LP(1)O9		1.97997	C1-C2	σ*	0.05489	2.06	1.23	0.045
			C2-N3	σ*	0.08612	0.64	1.01	0.023
			N12-H14	σ*	0.01535	1.00	1.19	0.031
LP(2)O9		1.87209	C1-C2	σ*	0.05489	12.00	0.78	0.088
			C1-N6	σ*	0.01551	0.63	0.86	0.021
			C2-N3	σ*	0.08612	25.54	0.57	0.109
			N12-N13	σ*	0.00845	0.93	0.74	0.024
			C12-H14	σ*	0.01535	2.27	0.75	0.038
LP(1)O11		1.98111	C1-C10	σ*	0.08789	1.64	1.05	0.038
			C10-N12	σ*	0.06848	1.32	1.03	0.033
LP(2)O11		1.86946	C1-C10	σ*	0.08789	19.18	0.60	0.096
			C10-N12	σ*	0.06848	22.63	0.57	0.103
LP(1)N12		1.81017	C10-O11	π *	0.23625	25.70	0.33	0.084
			N12-H14	σ*	0.01535	0.81	0.80	0.024
C1-N6	π *	0.19409	C10-O11	π *	0.23625	105.32	0.01	0.070
C2-O9	π *	0.30843	C1-N6	π *	0.19409	128.07	0.02	0.088
			N3-H15	σ*	0.01338	0.53	0.42	0.033

ED/e: Electron Density of donor and acceptor of NBO orbitals.

[a]*E(2)* means energy of hyper conjugative interaction (stabilization energy).

[b]*E(i) - E(j)* Energy difference between donor and acceptor i and j NBO orbitals.

[c]*F(i,j)* is the Fock matrix element between i and j NBO orbitals.

i: donor orbital; *j*: acceptor orbital; a.u: atomic unit; e: occupancy.

3.2 Local descriptor functions

The Fukui function is received as the local density functional descriptors to illustrate both chemical reactivity and selectivity. This local reactivity descriptor enables the regions where a chemical change will enhance its density when the number of electron changes. Accordingly, it indicates the propensity of the electronic density to deface at a specific locality about receiving or donating electrons [30]. The more compact or atomic Fukui functions of the jth atom positions are stated as per the following equations for an electrophilic $fj^-(r)$, nucleophilic and free radical attack $fj^+(r)$, fj^0 on the reference compound respectively

$$fj^+ = qj(N+1)-qj(N); \text{ for nucleophilic attack}$$
$$fj^- = qj(N)-qj(N-1); \text{ for electrophile attack}$$
$$fj^0 = \tfrac{1}{2}[\,qj(N+1)-qj(N-1)]; \text{ for radical attack}$$

Whereas, qj is the atomic charge at the jth atomic site in the corresponding neutral (N), anionic (N+1), or cationic (N-1) chemical species. It accommodates almost all the information concerning various global, local reactivity and discernment descriptors in addition to information about thr electrophilic or nucleophilic potential of the atomic site in a compound. The dual descriptor (Df(r)), defined as the difference between the nucleophilic and electrophilic Fukui function and is stated by
$$\Delta f(r) = [f^+(r)-f^-(r)]$$
The position is to recommend for a nucleophilic attack if $\Delta f(r)>0$. The site is recommended for the electrophilic attack if $\Delta f(r)<0$. Mathematic

descriptors $\Delta f(r)$ indicate a direct distinction between the nucleophilic and electrophilic attacks in a specified region [31]. The NBO charges have been described to be in tremendous acceptance for calculating Fukui functions [32]. From the **Table 4** it is coupled that the nucleophilic attacking sites for the tautomer **I** is C2 and N3, the electrophilic attacking sites are C9 and O13 and the radical attack sites for compound are O13 and C2. In tautomer - **II** nucleophilic attacking sites are C2, O9, the electrophilic attacking sites are O11, C2 and the radical attack sites for the compound are C2 and O11. The Fukui function has been indicated to be related to the local softness of a system. This property has permitted it to be used for biological applications involving ligand docking, active site detection, and protein folding.

The local softness condensed to an atom location described by $s^\pm_k = f\,k^\pm s$ [33] and local electrophilicity indices [34] defined by $\omega k^\pm = f\,k^\pm \omega$ is also calculated to describe the reactivity of atoms. These calculations estimate the most electrophilic site in a system has the highest value of s+ and ω+ while the highest value of s- and ω- analogous to the nucleophilic site in the compound. The local reactivity descriptors like $sk^{\pm 0}$, $\omega k^{\pm 0}$ furnish the reactivity propensity of the local site through nucleophilic or electrophilic attacks. The lower chemical hardness indicates a more stable nature of the molecule. The location of reactive electrophile sites and nucleophilic sites are in heeding with the whole electron density surface and chemical behavior.

Table 2. Local reactivity descriptors for Favipiravir tautomer - **I** and tautomer - **II** at B3LYP/6–311++G (d, p) level of theory

	Atom	$f^+(r)$	$f^-(r)$	$f^0(r)$	$\Delta f(r)$	Local hardness (au)	w^-(eV)	w^+(eV)
Tautomer - I	C1	0.0168	0.0039	0.0104	-0.0129	0.0001	0.0070	0.0300
	C2	0.5774	0.0002	0.2888	-0.5772	-0.0343	0.0003	1.0332

	N3	0.3928	0.0003	0.1965	-0.3925	-0.0233	0.0004	0.7029
	C4	0.0049	0.0002	0.0026	-0.0047	-0.0002	0.0004	0.0088
	C5	0.0007	0.0049	0.0028	0.0042	0.0014	0.0088	0.0013
	N6	0.0005	0.0092	0.0049	0.0087	0.0026	0.0165	0.0009
	H7	0.0000	0.0000	0.0000	0.0000	0.0000	0.0001	0.0000
	F8	0.0058	0.0000	0.0029	-0.0058	-0.0003	0.0000	0.0104
	C9	0.0004	0.0564	0.0284	0.0560	0.0160	0.1009	0.0007
	N10	0.0003	0.0178	0.0091	0.0175	0.0051	0.0319	0.0104
	H11	0.0001	0.0010	0.0005	0.0009	0.0003	0.0017	0.0001
	H12	0.0001	0.0034	0.0017	0.0033	0.0010	0.0060	0.0001
	O13	0.0001	0.9027	0.4514	0.9026	0.2574	1.6155	0.0002
	O14	0.0001	0.0000	0.0001	-0.0001	0.0000	0.0000	0.0003
	H15	0.0000	0.0000	0.0000	-0.0000	0.0000	0.0000	0.0000
Tautomer - I								
	C1	0.0712	0.0079	0.0395	0.0633	-0.0017	0.0130	0.1175
	C2	0.6180	0.0009	0.3095	0.6172	-0.0333	0.0015	1.0210
	N3	0.0195	0.0001	0.0098	0.0194	-0.0010	0.0002	0.0322
	C4	0.0178	0.0002	0.0090	0.0176	-0.0009	0.0003	0.0294
	C5	0.0093	0.0009	0.0051	0.0084	-0.0003	0.0015	0.0153
	N6	0.0029	0.0029	0.0029	0.0000	0.0006	0.0048	0.0048
	H7	0.0003	0.0000	0.0002	0.0003	0.0000	0.0000	0.0005
	F8	0.0002	0.0000	0.0001	0.0002	0.0000	0.0000	0.0003
	O9	0.2230	0.0000	0.1115	0.2230	-0.0121	0.0001	0.3684
	C10	0.0354	0.0233	0.0293	0.0121	0.0043	0.0384	0.0584
	O11	0.0001	0.9582	0.4792	-0.9581	0.2570	1.5830	0.0002
	N12	0.0011	0.0051	0.0031	-0.0039	0.0013	0.0084	0.0019
	H13	0.0000	0.0003	0.0002	-0.0002	0.0001	0.0004	0.0001
	H14	0.0009	0.0002	0.0006	0.0007	0.0000	0.0003	0.0016
	H15	0.0002	0.0000	0.0001	0.0002	0.0000	0.0000	0.0003

au: Atomic Unit.

eV: Electron volt.

3.3 APT charges

The atomic polarizability tensor (APT) charges are the amount of charge tensor and amount of charge flux tensor which is studied as charge-charge flux model [35]. The atomic charges relatively appear on the surface that could be present the whole chemical properties of the molecule [36-37].

The optimized geometrical structure and atomic polarizability tensor charges of tautomer - I and its tautomer – II is shown in **Table 5**. The atomic charges on the innumerable atomic site of tautomer - I and tautomer - II molecule have been calculated using the DFT/B3LYP/ with 6-311++G(d,p) level [38] and are

given in **Table 5** constitute the higher electronegativity in differentiation with the other atoms.

Here, the C2 atom exhibit the negative charge with magnitude -0.024 a.u., and the remaining four carbon atoms of the pyrazine ring C1, C3, C5, and C9 have a positive charge with magnitudes 0.529,0.623,0.128 and 1.185 a .u. respectively, but only the C2 atom of pyrazine ring atoms exhibit reactant property due to negative charge than other carbon atoms of the ring. The two atoms, O10, and O14 possess negative APT charges as -0.795 and -0.704 a.u. for the molecule. Analogous as the three atoms, N3, N6 and N11 have negative APT charges as -0.192,-0.306 and -0.756 a.u. of tautomer - **I**. The F8 atom has -0.593 a.u. due to the high electronegativity. In the molecule, the four H atoms (H7, H12, H13, and H15) of tautomer - **I** have positive APT charges with magnitudes 0.065, 0.282, 0.234, and 0.325 a.u. respectively.

The tautomer - **II** molecule, C1 and C9 atoms show the negative charge with magnitude -0.037a u. and -0.428 a.u. The remaining three carbon atoms of the pyrazine ring C2, C4, and C5 have positive charge with magnitudes 0.604, 0.084 and 0.390 a.u. respectively. The O14 atom possess negative APT charges as -0.628 and O10 atom possess positive APT -0.917 a.u. for the molecule. Analogous as the three atoms, N3, N6, and N11 have negative APT charges as -0.337, -0.083 and -0.764 a.u. of tautomer. The F8 atom has -0.712 a.u. due to the high electro negativity. In the molecule, the four H atoms (H7, H12, H13, and H15) of tautomer - **II** have positive APT charges with magnitudes 0.102, 0.241, 0.385, and 0.265 a.u. respectively. Also, it could be noticed that two of the H atoms (H12, H13) on Favipiravir molecule are attached directly toward the N atoms and have the positive APT charges, H15 directly attached towards the O atom, and H7 attached to pyrazine carbon.

Table 3. Calculated APT charges of Favipiravir tautomer - **I** and tautomer - **II** at B3LYP/6–311++G (d, p) level of theory.

S.no	Atom	APT Charges (a.u)	
		Tautomer - I	Tautomer - II
1	C1	0.529	-0.037
2	C2	-0.024	0.604
3	N3	-0.192	-0.337
4	C4	0.623	0.084
5	C5	0.128	0.390
6	N6	-0.306	-0.083
7	H7	0.065	0.102
8	F8	-0.593	-0.712
9	C9	1.185	-0.428
10	O10	-0.795	0.917
11	N11	-0.756	-0.764
12	H12	0.282	0.241
13	H13	0.234	0.385
14	O14	-0.704	-0.628
15	H15	0.325	0.265

a.u: AtomicUnit

3.4 AIM- NCI -RDG ANALYSIS.

The quantum theory of atoms in molecules (QTAIM), have been used to determine the intra and intermolecular hydrogen bond and to explore the bond structure of molecular systems [39-40]. The topological properties of the bond critical point (BCP) such as the electron density (ρ) as well Laplacian of electron density ($\nabla^2\rho$), Lagrangian kinetic electron density (g) and the potential electron density (v) have been investigated using the Baders theory, which is applied in AIMALL software [41].

Topological parameters such as Laplacian of electron density $\nabla^2\rho(r)$, the electron density $\rho(r)$, Lagrangian kinetic energy $G(r)$, the potential energy density $V(r)$, Hamiltonian kinetic energy can be used to view the of hydrogen bond properties within the molecule. $H(r) = G(r)+V(r)$, and the hydrogen bond energy (E_{HB}) can also be studied using QTAIM method as recommend by Espinosa et al. Eq. 1 estimate E_{HB} is the half of VBCP (1)

$$E_{HB} = ½ VBCP\ldots\ldots\ldots.. (1)$$

For AIM analysis, the optimized Favipiravir undergo intramolecular BCPs and ring critical points (RCPs). The calculation of AIM analysis was concluding using the Multiwfn program. The topological parameters of

Favipiravir the BCP are listed in **Table 6**. According to Rozas et al. [42], the hydrogen bond interactions can be classified as follows:

(1) Weak hydrogen bonds are detected by $\nabla^2\rho(r) > 0$ and $H(r) >0$

(2) Moderate hydrogen bonds are detected by $\nabla^2\rho(r) > 0$ and $H(r) < 0$

(3) Strong hydrogen bonds are detected by $\nabla^2\rho(r) < 0$ and $H(r) < 0$

Electron density $\rho(r)$ and its Laplacian $\nabla^2\rho(r)$ assist to calculate the nature of interactions. Normally the huge values of electron density $\rho(r)$ and its Laplacian $\nabla^2\rho(r)$ show the potentiality of hydrogen interactions [43]. The positive values of Laplacian $\nabla^2\rho(r)$ are assign to the reducing of the charge in the internuclear region, while the negative values are provocative of a strong covalent character. From **Table 6**, we observed N11-H12…O14 and N12-H14…O9 type of interaction, where the electron density values are 0.02 a.u.,0.27a.u. and the values of Laplacian are 0.10 a.u., 0.14 a.u. respectively. As known, positive values of Laplacian $\nabla^2\rho(r)$ and low values of electron density $\rho(r)$ in BCPs suggested the presence of hydrogen bond interactions [44]. The intramolecular interaction energy at BCP shows one O…H intramolecular hydrogen bonding the bond energy of both the Favipiravir tautomers have been calculated as -13.12 kJ/mol.

Table 4. Topological parameters for bonds of interacting atoms Favipiravir tautomer - **I** and tautomer - **II**: electron density (ρr), Laplacian of electron density ($\nabla^2\rho r$), electron kinetic energy density (G), electron potential energy density (V), total electron energy density (H) at bond critical point (BCP)

S.no	Bond	$\rho(r)$	$\nabla^2\rho(r)$	G	V	H	E_{HB}
Tautomer - I							
1	C1-C2	0.30	-0.82	0.09	-0.40	-0.31	
2	C2-N3	0.33	-0.87	0.26	-0.75	-0.49	
3	N3-C4	0.37	-1.08	0.28	-0.84	-0.56	
4	C5-N6	0.34	-0.88	0.27	-0.77	-0.50	

5	C4-C5	0.31	-0.90	0.10	-0.43	-0.33	
6	C1-N6	0.35	-1.07	0.23	-0.73	-0.50	
7	C5-H7	0.28	-1.01	0.03	-0.31	-0.28	
8	C4-F8	0.26	0.03	0.35	-0.71	-0.36	
9	C2-C9	0.24	-0.58	0.05	-0.25	-0.20	
10	C9-O10	0.41	-0.26	0.63	-1.33	-0.70	
11	H12-O14	0.02	0.10	0.02	-0.01	0.01	-13.12
12	C9-N11	0.31	-0.92	0.20	-0.64	-0.44	
13	N11-H12	0.33	-1.72	0.05	-0.53	-0.48	
14	C1-O14	0.29	-0.44	0.31	-0.73	-0.42	
15	N11-H13	0.33	-1.66	0.05	-0.51	-0.46	
16	O14-H15	0.35	-2.52	0.06	-0.76	-0.70	
Tautomer - II							
	C1-C2	0.30	-0.99	0.05	-0.36	-0.21	
	C2-N3	0.26	-0.76	0.06	-0.31	-0.25	
	N3-C4	0.26	-0.73	0.07	-0.33	-0.26	
	C5-N6	0.27	-0.74	0.06	-0.32	-0.26	
	C4- C5	0.32	-0.92	0.12	-0.48	-0.36	
	C1-N6	0.36	-0.79	0.36	-0.93	-0.57	
	C4-H7	0.29	-1.05	0.03	-0.32	-0.29	
	C5-F8	0.25	-0.01	0.33	-0.68	-0.35	
	C2-O9	0.36	-0.41	0.47	-1.05	-0.58	
	C1-C10	0.24	-0.57	0.05	-0.21	-0.18	
	C10-O11	0.36	-0.42	0.47	-1.05	-0.58	
	C10-N12	0.26	-0.75	0.05	-0.30	-0.25	
	O9-H14	0.27	+0.14	0.03	-0.20	0.01	-13.12
	N12-H13	0.35	-1.77	0.05	-0.55	-0.50	
	N12-H14	0.35	-1.83	0.05	-0.56	-0.51	
	N3-H15	0.35	-1.87	0.05	-0.58	-0.53	
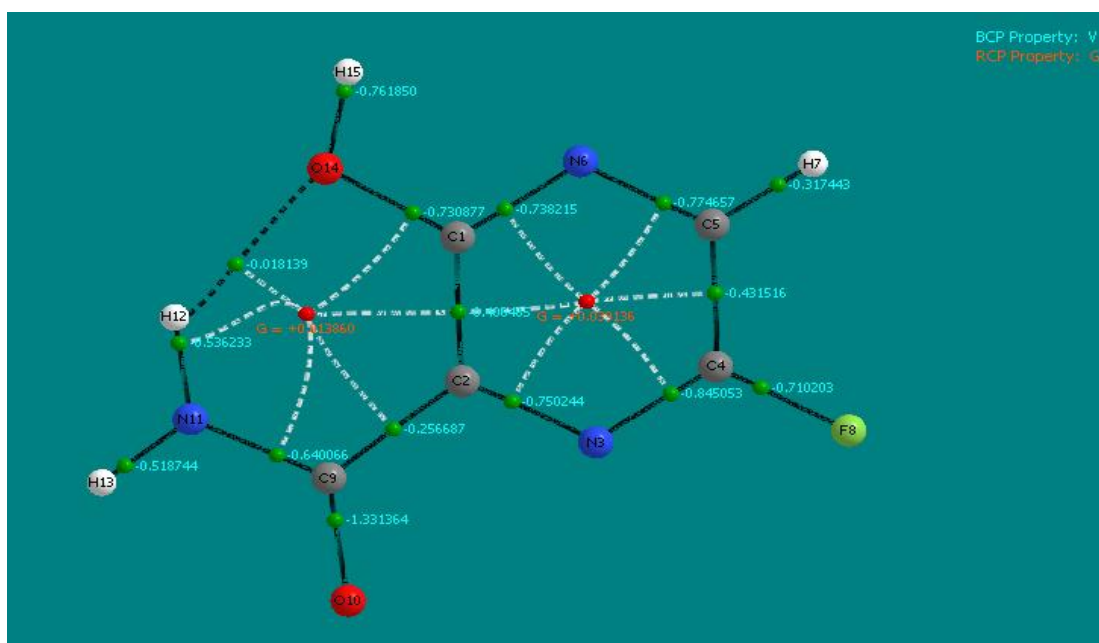
3(a)
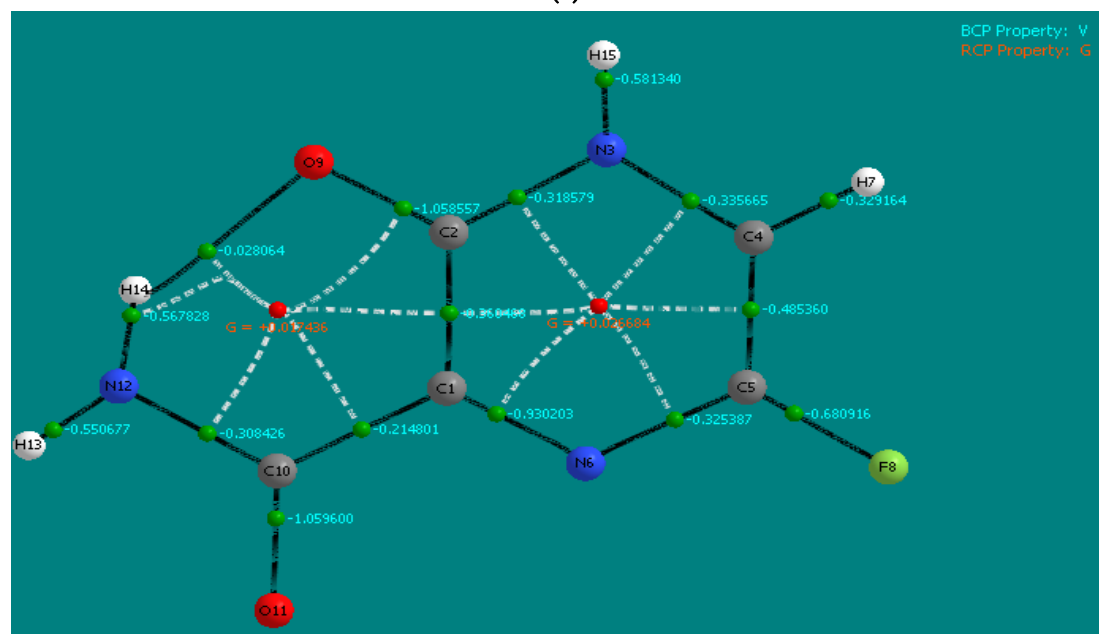
3(b)

Fig.3. AIM molecular graphs of Favipiravir tautomer - **I (3a)** tautomer - **II (3b)** (RCP is shown as small red spheres, BCP is shown as small green spheres, Hydrogen bond show doted lines).

The NCI analysis indicates constructive information about the noncovalent interactions within a molecule. The strong directional attractions correlated with localized atom-atom contacts and the molecular division having weak interactions can be illustrious by an NCI plot. The reduced density gradient (RDG) is an inceptive non-dimensional quantity, which implicates the density and first derivative, and it is illuminated by the formula following [45].

$$RDG(r) = \frac{1}{2(3\pi^2)^{1/3}} \frac{|\nabla\rho(r)|}{\rho(r)^{4/3}}$$

The scatter graphs plotted reduced density gradient against electron density r, arrangement by the sign of λ_2 and the 3D color-filled reduced density gradient isosurface are appear in **Fig 5(a), 5(b), 6(a), and 6(b).**

From the graph, it can be seen that weak forces of interaction are current between the atoms in the molecule. The NCI index provides more confirmation of noncovalent interaction, and it is built upon the reduced density gradient (RDG). The electron density quantity of the RDG against sign (λ_2) ρ peaks gives us statistics about the nature and power of interactions of molecules. The interaction of the power in the molecular system, which designates the stronger advisability of blue color and the push of red, is studied with Multiwfn and VMD software.

The value of sign (λ_2) ρ is particularly important in the nature of the interaction. It means if the sign (λ_2) ρ > 0 indicates a repulsive interaction (non-bonded) and the sign (λ_2) ρ < 0 shows an attractive interaction (bonded).

The RDG scatter graphs of tautomer - **I** and tautomer - **II** on the left side the blue colors indicate the hydrogen-bonding interaction, green colors are van der Waals interactions, and the red color is illustrated as strong repulsion (steric effect). When looking at tautomer - **I**, hydrogen-bonding interactions were more.
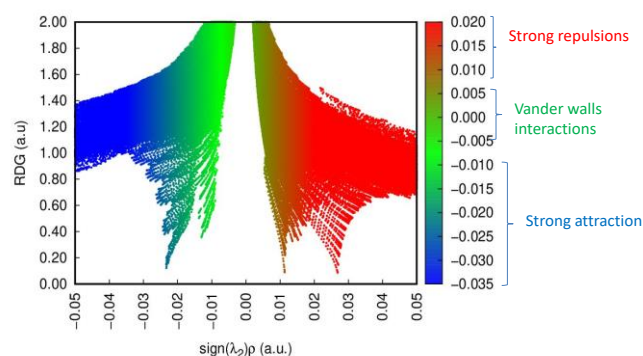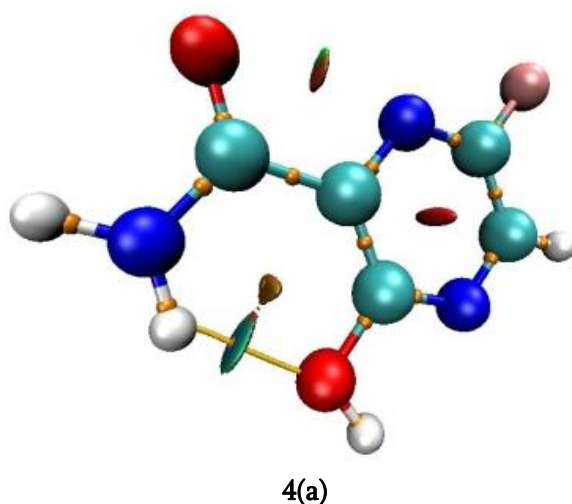
4(b)

Fig. 4. Non- covalen interaction **4(a)** and Reduced density gradient (RDG) analysis **4(b)** to identify weak and strong interaction in Favipiravir tautomer – **I**

5(a)
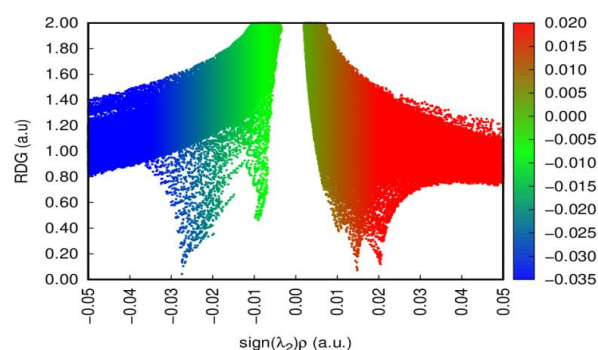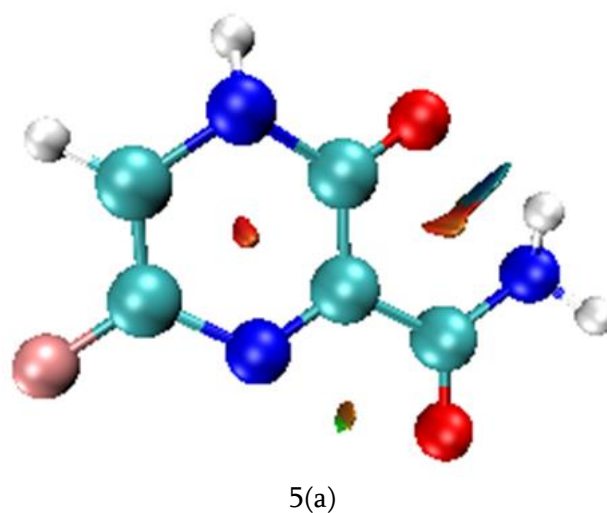
5(b)

Fig. 5. Non - covalen interaction **5(a)**, and Reduced density gradient (RDG) analysis **5(b)** to identify weak and strong interaction in tautomer - **II**.

4(a)

3.5 Potential energy surface scan (PES) analysis

The potential energy surface scan is used to illustrate the relationship between potential energy and molecular geometry [46]. For tautomer - **I** the minimum energy distribution was obtained by PES scan analysis by choosing the dihedral angle C1-C2-C9-N11. This dihedral angle is also applicable co-ordinate for conformational flexibility within the molecule. The determined dihedral angle range from 0° to 360° rotations by a step of 10°. The lowest global minimum energy is obtained at 175° in the potential energy curve with an energy value -381320.432 kJ/mol, which is due to the possibility of strong N11-H12...O14 hydrogen bonding as supported by NBO analysis. The maximum energy value -381320.44 kJ/mol obtained at 350°. The separation between the energy curves shows the highest potential barrier $\Delta E = 8$ kJ/mol.
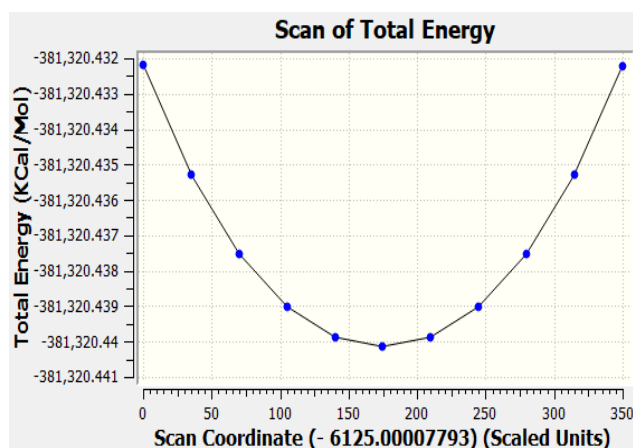
Fig. 6. Potential energy surface scan of Favipiravir tautomer - **I**.

3.6 Bioactivity and toxicity risk studies

The prediction of bioactivity and toxicity risk studies of **1-4** compounds (**Table 9**) revealed their bioactivity properties like GPCR ligand property, ion channel modulator, kinase inhibitor, nuclear receptor-ligand interactions, protease inhibitor, enzyme inhibitor interactions, and drug properties like drug-likeness, and drug scores have studied and find out potential non-toxic molecules. This Molinspiration prediction extensively assist to investigate the cheminformatics of the compounds under analysis by correlating with the database of in vitro and in vivo studies of accepted drugs based on mutual functional group comparison. The toxicity risk results plainly indicate that **1-4** compounds are safer as exhibit low or no risks of mutagenicity, tumorigenicity, irritant and low or no effect on the reproductive system and obeys drug-like behavior. The positive value of drug-likeness states that the molecule contains predominantly fragments that are frequently present in commercial drugs. Solubility is an important factor that aids in the movement of the compound from the site of administration into the bloodstream and poor solubility leads to poor absorption. Alike drug score is a harmonizing parameter of drug-likeness, ClogP, logS, molecular weight and toxicity risks and used to judge the compound's overall potential to qualify for a drug. Ultimately it is predicted that all the compounds **1-4** exhibited higher scores.

Table 5. Bioactivity scores of **1-4** compounds.

Parameter		1	2	3	4
Bioactivity	GPCRL	-0.43	-0.62	-0.35	-0.60
	ICM	0.42	-0.44	0.39	0.41
	KI	-0.35	-0.31	-0.15	-0.36
	NRL	-1.14	-1.50	-1.20	-1.18
	PI	-0.58	-0.91	-0.60	-0.90
	EI	-0.18	-0.33	-0.13	-0.18
Toxicity risks	Mut	Nil	Nil	Nil	Nil
	Tum	Nil	Nil	Nil	Nil
	Irrit	Nil	Nil	Nil	Nil
	R.E	Nil	Nil	Nil	Nil

GPCRL: G protein-coupled receptor ligand.

ICM: Ion channel modulator; KI: Kinase inhibitor.

NRL: Nuclear receptor ligand.

PI: Protease inhibitor.

EI: Enzyme inhibitor.

Mut: Mutagenic.

Tum: Tumorigenic.

Irrit: Irritant.

R.E: Reproductive efect.

3.7 Molecular docking studies

Molecular docking is used to predict the classic binding direction, affinity, and activity of drug molecules and their protein targets. The title molecule was chosen to be docked into the active sites of the protein 5R7Y. This protein is obtained from a protein data bank (PDB ID:5R7Y). Molecular docking study has been carried out by Gaussian, optimized tautomer - **I** and tautomer - **II** molecule as a ligand with selected proteins using Auto dock 4.2.6, Autogrid 4.0 software. Atomic charges were determined using the Kollmann and Gasteiger method after adding the polar hydrogen. The active site of the protein was defined with 40Å x 40Å x 40Å grid size, with the Lamarkkian Genetic Algorithm (LGA) being used to carry out the process. The minimum binding energies of tautomer - **I** is obtained to be -3.9 kcal/mol. It shows three interactions are formed between Tyr126, Val125, and Aal7 and one intramolecular hydrogen bond of receptor moiety. The bond distances are 3.46 Å, 5.36 Å, 2.20 Å, and 1.98 Å. Tautomer - **II** show -4.62 kcal/mol of minimum binding energy, and two interactions are formed between Aal7, Gln127, one intramolecular hydrogen bond of receptor moiety. The bond distances are 1.99 Å, 2.96 Å and 1.98 Å. In this endeavor, it was confirmed that the Favipiravir molecule is a stimulate aspirant of COVID-19 symptomatic.

Table 6. The binding affinity values of Favipiravir tautomer - **I** and tautomer – **II** predicted by Autodock 4.2.6.

Protein (PDB ID)	Binding Energy	Reference RMSD	Estimated Inhibition Constant
5R7Y tautomer - **I**	-3.9 kcal/mol	26.15 A⁰	1.69 μm
5R7Y tautomer - **II**	-4.62 kcal/mol	19.59 A⁰	413.84 μm
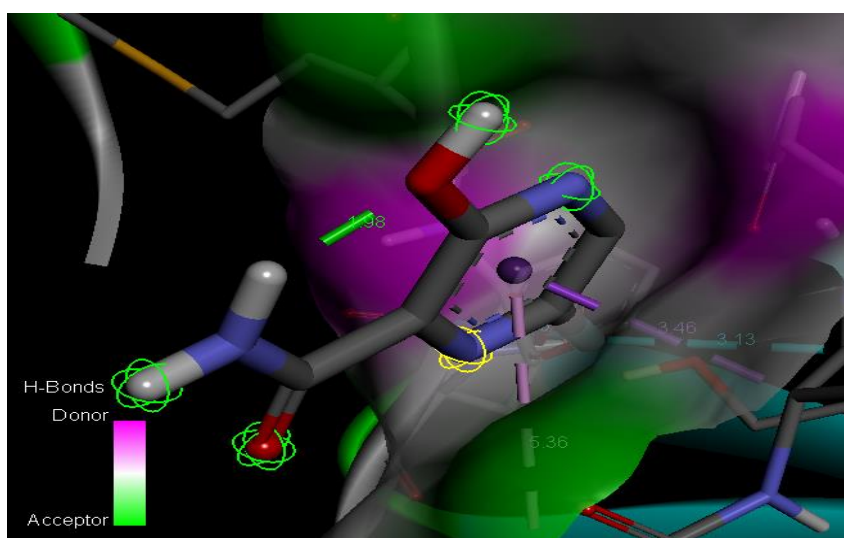
Fig. 7(a). Hydrogen bonding interactions between Favipiravir tautomer - **I** and target protein (PDB ID: 5R7Y).
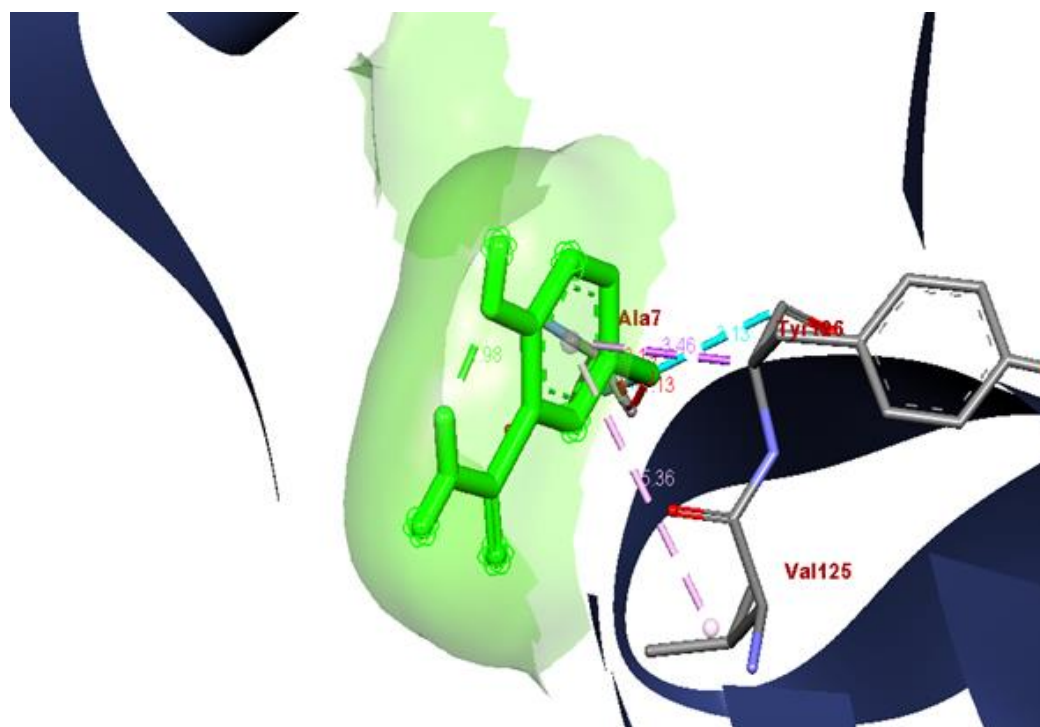
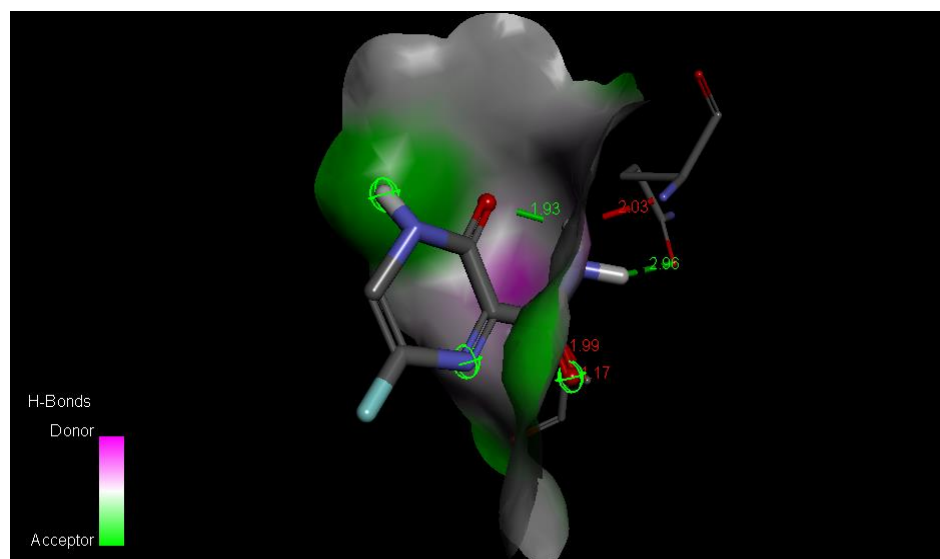**Fig. 7(b).** Amino acids interactions between Favipiravir tautomer - **I** and target protein (PDB ID: 5R7Y).

Fig. 8(a). Hydrogen bonding interactions between tautomer - **II** and target protein (PDB ID: 5R7Y).
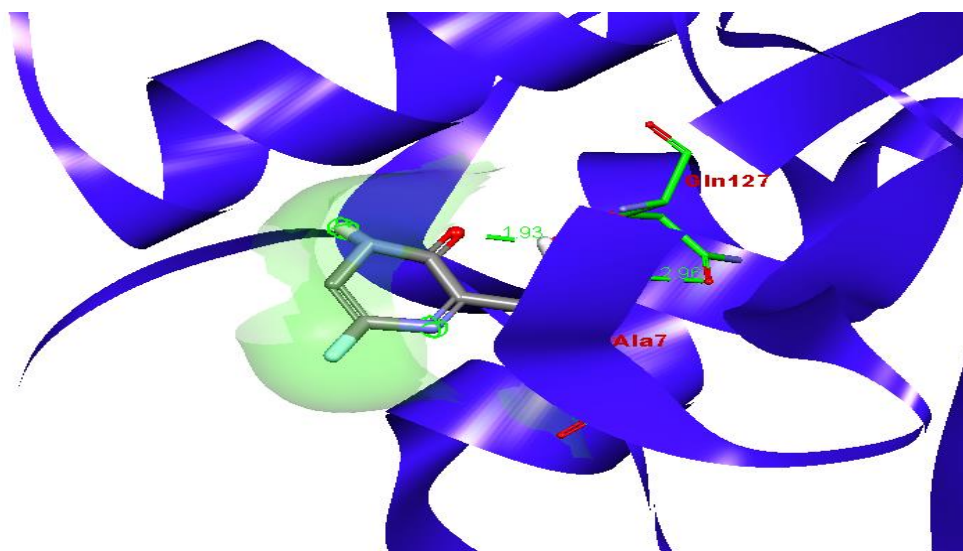
.

Fig. 8(b). Amino acids interactions between tautomer - **II** and target protein (PDB ID: 5R7Y)

IV. CONCLUSION

In this, theoretical study of Favipiravir tautomer molecules, the DFT calculations have been analyzed using B3LYP/6-311++G (d, p). The π*→π* transitions have the highest resonance energies relative to the other interactions of the title molecule from the results of the NBO analysis. APT charges, and local reactivity descriptors are analyzed in tautomer – **I** and tautomer - **II** molecules. In QTAIM, the interaction energy at BCP shows one (N-H…O) intermolecular hydrogen bonding (H12…O14) in tautomer - **I**, the bond energy is calculated as -13.12 kJ/mol, and in tautomer- **II** intermolecular hydrogen bonding (N12-H14…O9), the bond energy is calculated as -13.12 kJ/mol. The interactions formed within the molecule, such as Van der Walls, hydrogen bond interactions, and steric effects are classified by the means of RDG surface analysis. The maximum energy value was found to be -381320.44 kJ/mol using a potential energy surface scan study. Bioactivity properties are analyzed. **1-4** molecules show good pharmacokinetic properties. Molecular docking simulations have been concluded.

Conflicts of inerest/Competing interests: No potential conflict of interest was reported by the authors

Availability of data and material: All data and material (used herein) are available.

Code availability: Not applicable

Author's Contribution: Both the authors (N. Kavitha and M. Alivelu) have participated in conception and design, analysis and interpretation of the data, drafting the article and approval of the final version.

V. REFERENCES

[1]. M. Lipsitch, DL. Swerdlow, L. Finelli, Defining the epidemiology of Covid-19 - studies needed. New Engl. J. Med. 382 (13) (2020) 1194-1196, https://doi.org/10.1056/NEJMp2002125.

[2]. L. Oehninger, R. Rubbiani, I. Ott, N-Heterocyclic carbene metal complexes in medicinal chemistry. Dalton Trans. 42 (2013) 3269–3284, https://doi.org/10.1039/C2DT32617E.

[3]. H.-H. Gong, D. Addla, J.-S. Lv, C.-H. Zhou, Heterocyclic naphthalimides as new skeleton structure of compounds with increasingly

expanding relational medicinal applications. Curr. Top. Med. Chem. 16 (28) (2016) 3303–3364, https://doi.org/10.2174/15680266166661605061 45943.

[4]. I.V. Ukrainets, N.L. Bereznyakova, Heterocyclic diuretics, Chem. Heterocycl. Compd. 48 (1) (2012) 155-165, https://doi.org/10.1007/s10593-012-0979-1.

[5]. P.B. Miniyar, P.R. Murumkar, P.S. Patil, M.A. Barmade, K.G. Bothara, Unequivocal role of pyrazine ring in medicinally important compounds: a review, Mini Rev. Med. Chem. 13 (11) (2013) 1607-1625, https://doi.org/10.2174/1389557511313110007.

[6]. S. Martin, C. Revathi, D. Dayalan, N. Mathivannan, V. Shanmugaiya, Halocobaloximes containing coordinated pyrazine, pyrazine carboxylic acid and pyrazine carboxamide: Microwave assisted synthesis, characterization and antibacterial activity, Rasayan J. Chem. 1 (2) (2008) 378-389.

[7]. K. Konno, F.M. Feldmann, W. McDermott, Pyrazinamide susceptibility and amidase activity of tubercle bacilli, Am. Rev Respir Dis. 95(3) (1967) 461-469, https://doi.org/ 10.1164/arrd.1967.95.3.461.

[8]. Y. Zhang, M.M. Wade, A. Scorpio, H. Zhang, Z. Sun, Mode of action of pyrazinamide: disruption of Mycobacterium tuberculosis membrane transport and energetics by pyrazinoic acid, J. Antimicrob. Chemotherapy 52 (5) (2003) 790-795, https://doi.org/10.1093/jac/dkg446.

[9]. Y. Furuta, BB. Gowen, K. Takahashi, K. Shiraki, DF. Smee, DL. Barnard, Favipiravir (T-705), a novel viral RNA polymerase inhibitor, Antivir. Res. 100 (2) (2013) 446-454, https://doi.org/ 10.1016/j.antiviral.2013.09.015.

[10]. M. Kiso, K. Takahashi, Y. Sakai-Tagawa, K. Shinya, S. Sakabe, Q.M. Le, M. Ozawa, Y. Furuta, Y. Kawaoka, T-705 (Favipiravir)

activity against lethal H5N1 influenza A viruses. Proc. Nat. Acad. Sci. 107 (2) (2010) 882-887, https://doi.org/ 10.1073/pnas.0909603107.

[11]. Q. Cai, M. Yang, D. Liu, J. Chen, D. Shu, J. Xia, X. Liao, Y. Gu, Q. Cai, Y. Yang, C. Shen, Experimental treatment with Favipiravir for COVID-19: An open-label control study, Engineering, 6 (10) (2020) 1192-1198, https://doi.org/10.1016/j.eng.2020.03.007.

[12]. N. Kavitha, and M. Alivelu, "Investigation of Structures, QTAIM, RDG, ADMET, and Docking properties of SASC Compound using Experimental and Theoretical Approach," Computational and Theoritical Chemistry 1201 (2021): 113287, https://doi.org/10.1016/j.comptc.2021.113287.

[13]. N. Kavitha, and M. Alivelu, R. Konakanchi, Computational Quantum Chemical Study, Insilco ADMET, and Molecular Docking Study of 2-Mercapto Benzimidazole, Polycyclic Aromatic Compounds 2021, https://doi.org/10.1080/10406638.2021.1939071.

[14]. M. Hagar, H.A. Ahmed , G. Aljohani , O.A. Alhaddad, Investigation of Some Antiviral N-Heterocycles as COVID 19 Drug: Molecular Docking and DFT Calculations, Int. J. Mol. Sci. 21 (11) (2020) 3922. https://doi.org/10.3390/ijms21113922.

[15]. H. Sayiner, Serap SENTURK DALGIC, and FATMA KANDEMIRLI, DFT Based Quantum Chemical Descriptors of Favipiravir Forms, Authorea, May 29, 2020 https://doi.org/ 10.22541/au.159077082.27222996.

[16]. P. Yadav, P. Chowdhury, Repurposing the Combination Drug of Favipiravir, Hydroxychloroquine and Oseltamivir as a Potential Inhibitor against SARS CoV-2: A Computational Study, arXiv, 2020. PPR: PPR272833.

[17]. M.J. Frisch, G.W. Trucks, H.B. Schlegel, Gaussian 09W Program, Gaussian Inc., Wallingford, CT, 2009.

[18]. A.D. Becke, Density functional thermo chemistry. III. The role of exact exchange, J. Chem. Phys. 98 (1993) 5648-5652. https://doi.org/10.1063/1.464913.

[19]. A.D. Becke, Density-fnnctional exchange-energy approximation with correct asymptotic behavior, Phys. Rev. A 38 (1988) 3098-3100, https://doi.org/10.1103/PhysRevA.38.3098.

[20]. S. Shahab, M. Sheikhi, L. Filippovich, D.E. Anatol'evich, H.Yahyaei, Quantum chemical modeling of new derivatives of (E,E)-azomethines: Synthesis, spectroscopic (FT-IR, UV/Vis, polarization) and thermophysical investigations, J. Mol. Struct., 1137 (2017) 335-348,
https://doi.org/10.22631/chemm.2017.96853.1009.

[21]. R. Bader, Atoms in Molecules: A Quantum Theory, Oxford University Press, USA, 1994.

[22]. T. Lu, F. Chen, Multiwfn: a multifunctional wave function analyzer. J. Comput. Chem. 33(5) (2012):580–592, https://doi.org/10.1002/jcc.22885.

[23]. E. Runge, E.K.U. Gross, Density-functional theory for time dependent systems. Phys. Rev. Lett. 52 (12) (1984) 997. //doi.org/10.1103/PhysRevLett.52.997.

[24]. W. Humphrey, A. Dalke, K. Schulten VMD: visual molecular dynamics. J. Mol. Graph. 14 (1) (1996) 33–38, https://doi.org/10.1016/0263-7855 (96)00018-5.

[25]. G.M. Morris, R. Huey, A.J. Olson, Using AutoDock for ligand-receptor docking, Curr. Protoc. Bioinf. 24 (8.14) (2008) 8.14.1- 8.14.40, https://doi.org/10.1002/0471250953.bi0814s24.

[26]. D. Systemes, BIOVIA, Discovery Studio Modeling Environment. Release 4.5, Dassault Systemes: San Diego, CA. (2015).

[27]. E.D. Glendening, A.E. Reed, J.E. Carpenter, F. Weinhold, NBO Version 3.1, TCI, University of Wisconsin, Madison, 1998.

[28]. D. Jacquemin, J. Preat, E.A. Perpete, A TD-DFT study of the absorption spectra of fast dye salts, Chem. Phys. Lett. 410 (2005) 254-259, https://doi.org/10.1016/j.cplett.2005.05.081.

[29]. A.E. Reed, L.A. Curtiss, F. Weinhold, Intermolecular Interactions from a Natural Bond Orbital, Donor-Acceptor Viewpoint, Chem. Rev. 88 (1988) 899-926, https://doi.org/10.1021/cr00088a005.

[30]. R. K. Roy, H. Hirao, S. Krishnamurthy, S. Pal, Mulliken population analysis based evaluation of condensed Fukui function indices using fractional molecular charge, J. Chem. Phys. 115 (7) (2001) 2901-2907 https://doi.org/10.1063/1.1386699.

[31]. C. Morell, A. Grand, A. Toro-Labbe, New dual descriptor for chemical reactivity, J. Phys. Chem., 109 (1) (2005) 205-212, https://doi.org/10.1021/jp046577a.

[32]. F. Nazari, F.R. Zali, Density functional study of the relative reactivity of the carbonyl group in substituted cyclohexanone, J. Mol. Struct. (Theochem) 817 (2007) 11-18. https://doi.org/10.1016/j.theochem.2007.04.013.

[33]. C. Lee, W. Yang, R.G. Parr, Local softness and chemical reactivity in the molecules CO, SCN- and H2CO*, J. Mol. Struct. (Theochem) 163 (1988) 305-313. https://doi.org/10.1016/0166-1280(88)80397-X.

[34]. R.M. Silverstein, F.X. Webster, D.J. Kiemle, Spectrometric identification of organic compounds, 7th edition, USA, (2005).

[35]. M.M.C. Ferreira, E. Suto, Atomic polar tensor transferability and atomic charges in the fluoromethane series CHxF4-x, J. Phys. Chem. 96 (22) (1992), 8844-8849, https://doi.org/10.1021/j100201a030.

[36]. M.J.S. Dewar, The Molecular Orbital Theory of Organic Chem (Mc. Graw- Hill and Inc., New York, 1969, https://doi.org/10.1002/ange.19700820418.

[37]. C.A. Coulson, R. McWeeny, Coulson's Valence (Oxford University Press, Oxford, 1979).

[38]. M.J. Frisch et al., Gaussian 09, Revision C.01 (G. Inc., Wallingford, 2010)

[39]. R.F.W. Bader, Atoms in Molecules-A Quantum Theory, Oxford University Press, Oxford, 1990.

[40]. P.-D.A. Savin, R. Nesper, S. Wengert, T. F. Fassler, ELF: The electron localization function, Angew. Chem. Int. Ed. Engl. 36 (17) (1997) 1808-1832, https://doi.org/10.1002/anie.199718081.

[41]. T. Keith, Aimall (Version 13.02.26), Tk Gristmill software (2012).

[42]. I. Rozas, I. Alkorta, J. Elguero Behavior of ylides containing N, O, and C atoms as hydrogen bond acceptors, J. Am. Chem. Soc. 122 (45) (2000) 11154–11161, https://doi.org/10.1021/ja0017864.

[43]. E.R. Johnson, S. Keinan, P. Mori-Sánchez, J. Contreras-García, A.J. Cohen, W. Yang Revealing noncovalent interactions. J. Am. Chem. Soc. 132 (18) (2010) 6498–6506, https://doi.org/10.1021/ja100936w.

[44]. Bader RFW Atoms in molecules – a quantum theory. Oxford University Press, Oxford, 1990.

[45]. P. Agarwal, S. Bee, A. Gupta, P. Tandon, V.K. Rastogi, S. Mishra, P. Rawat, Quantum chemical study on influence of intermolecular hydrogen bonding on the geometry, the atomic charges and the vibrational dynamics of 2,6-dichlorobenzonitrile, Spectrochim. Acta A Mol. Biomol. Spectrosc. 121 (2014) 464–482, https://doi.org/10.1016/j.saa.2013.10.104.

[46]. G.P Sheeja Mol, D. Aruldhas, I. Hubert Joe, S. Balachandran, Spectroscopic investigation, fungicidal activity and molecular dynamics simulation on benzimidazol-2- yl carbamate derivatives, J. of Mol. Struc. 1176 (2019) 226–237, https://doi.org/10.1016/j.molstruc.2018.08.092.

Cite this article as :